J. Eukaryot. Microbiol., 53(3), 2006 pp. 165–176

DOI: 10.1111/j.1550-7408.2006.00090.x

Development of the Insect Pathogenic Alga *Helicosporidium*

VERENA-ULRIKE BLÄSKE-LIETZE,[a] ALEXANDRA M. SHAPIRO,[b] JOHN S. DENTON,[c] MICHAEL BOTTS,[a]
JAMES J. BECNEL[b] and DRION G. BOUCIAS[a]

[a]*Department of Entomology and Nematology, University of Florida, Gainesville, Florida 32611, and*
[b]*Center for Medical, Agricultural and Veterinary Entomology, USDA ARS, Gainesville, Florida 32604, and*
[c]*Harvard University, Cambridge, Massachusetts 02138*

ABSTRACT. This study examined the morphogenesis and replication dynamics of the different life stages (cysts, filamentous cells, vegetative cells) of *Helicosporidium* sp., a non-photosynthetic, entomopathogenic alga. The isolate (SjHe) used originated from an infected black fly larva. Filamentous cell transformation into vegetative cells and autosporulation during vegetative cell replication were observed under controlled in vitro conditions. The transformation process was initiated by a partial swelling of the filamentous cell along with the reorganization of the nuclear material. Two subsequent nuclear and cell divisions resulted in the release of 4 rod-shaped daughter cells, which divided into oval to spherical vegetative cells. These underwent several cycles of autosporogenic cell division. Multiple-passaged vegetative cell cultures formed non-motile, adherent cell clusters (palmelloid colonies). Vegetative replication dynamics were also observed in 2 experimental noctuid hosts, *Spodoptera exigua* and *Helicoverpa zea*. The average density of helicosporidial cells produced per microliter hemolymph exceeded cell concentrations obtained in vitro by 15- and 46-fold in *S. exigua* and *H. zea*, respectively. Cyst morphogenesis was only observed in the hemolymph, whereas no cysts differentiated at various in vitro conditions.

Key Words. Cyst morphogenesis, entomopathogenic alga, filamentous cell transformation, in vitro replication dynamics, Noctuidae.

THE protist *Helicosporidium* sp. (Chlorophyta: Trebouxiophyceae) is an achlorophyllous, entomopathogenic alga that has retained a modified but functional plastid genome (Tartar and Boucias 2004). Twenty nucleus-encoded, putatively plastid-targeted enzymes involved in various metabolic pathways have recently been identified in an expressed sequence tag survey (de Koning and Keeling 2004). However, because of their cryptic nature, plastids have not been visually detected in ultrastructural studies of this organism (Yaman and Radek 2005). Since the first description of *Helicosporidium* by Keilin (1921), this highly adapted, hemolymph-borne pathogen has been found to infect a variety of insects within the orders Diptera, Coleoptera, and Lepidoptera (Bläske and Boucias 2004; Boucias et al. 2001; Chapman, Woodward, and Petersen 1967; Conklin et al. 2005; Fukuda, Lindegren, and Chapman 1976; Hembree 1979; Lindegren and Okumura 1973; Purrini 1980, 1985; Seif and Rifaat 2001; Weiser 1970; Yaman and Radek 2005). To date, different species of *Helicosporidium* could not be identified from the available morphological data, and molecular data suggest that infections found in the various hosts represent different isolates or strains of the originally described species, *Helicosporidium parasiticum* (Keilin 1921; Tartar et al. 2003; Yaman and Radek 2005). This parasite is characterized by an infectious cyst stage that contains within a pellicle an elongate filamentous cell and 3 ovoid cells. Following ingestion, the cyst dehisces within the midgut lumen of the host and releases the invasive filamentous cell, which then penetrates the columnar epithelium and enters the hemocoel (Bläske-Lietze and Boucias 2005). The filamentous cells possess characteristic surface projections (barbs) that have been hypothesized to mechanically aid in the passage through the midgut epithelial layer (Boucias et al. 2001). Within the nutrient-rich hemolymph, *Helicosporidium* undergoes multiple cycles of vegetative replication. Like the cyst stage, vegetative cells are non-motile and enclosed within a pellicle, which can contain 1, 2, 4, or 8 daughter cells (Boucias et al. 2001; Lindegren and Hoffmann 1976). Eventually, the host hemocoel is colonized by massive numbers of vegetative cells, a portion of which differentiate into mature cysts. The resulting in vivo cells can be harvested and cultured in vitro (Boucias et al. 2001). Purified in vivo-produced cysts can be experimentally dehisced with larval digestive fluids from different lepidopteran species (Boucias et al. 2001).

In the present study, methods were developed to produce purified preparations of *Helicosporidium* filamentous cells and vegetative cells, thus allowing observations of the different cell phenotypes under controlled in vitro conditions. The SjHe isolate of *Helicosporidium* was used for all experiments. In vitro replication dynamics were compared with replication rates and cell development in 2 noctuid hosts. Most importantly, the filamentous cell transformation into vegetative cells was described for the first time.

MATERIALS AND METHODS

Insects and *Helicosporidium* cyst preparations. Eggs of *Heliocoverpa zea* Boddie and *Spodoptera exigua* Hübner (Lepidoptera: Noctuidae) were purchased from the United States Department of Agriculture, Agricultural Research Service, Southern Insect Management Research Unit, Stoneville, MS. Neonates and larvae were provided with a wheat germ-based, semi-synthetic insect diet containing antimicrobial agents and preservatives (Shorey and Hale 1965). Insects were maintained at constant conditions (26 °C ± 1 °C, 70% ± 5% RH, 12-h photoperiod). The SjHe isolate of *Helicosporidium* (ATCC 50920) used in this study originated from an infected black fly larva, *Simulium jonesi* Stone & Snoddy (Diptera: Simuliidae), collected from Hatchet Creek, Alachua County, FL. On a 4-wk basis, cysts were propagated by hemocoelic injection into fifth instar larvae of *H. zea*. Larvae were provided with diet ad libitum and incubated for 3 wk at constant conditions (26 °C ± 1 °C, 70% ± 5% RH, 12-h photoperiod). Cysts were then purified from homogenates of infected pupae by centrifugation (1,400 *g* for 45 min) on a 5–60% linear gradient of aqueous Ludox HS-40 (Sigma, St. Louis, MO). The band at a density of 1.16 g/ml, which contained the cysts, was collected, diluted in sterilized water, and subjected to several cycles of centrifugation (700 *g* for 10 min) to remove residual gradient material. After resuspension in sterilized water, purity of the suspension was checked by light microscopic observation. Cysts were counted using a hemocytometer and stored at 4 °C.

***Helicosporidium* filamentous cell preparations.** To prepare filamentous cell suspensions, in vivo-produced cysts were experimentally dehisced with digestive fluids harvested from *H. zea* or *S. exigua*. To obtain digestive fluids, digestive tracts were dissected on ice from late instar larvae and collected into

Corresponding Author: V.-U. Bläeske-Lietze, Department of Entomology and Nematology, University of Florida, Gainesville, FL 32611—Telephone number: 352-392-1901, ext. 202; FAX number: 352-392-0190; e-mail: vblaeske@ufl.edu

microcentrifuge tubes. After centrifugation at 2,000 *g* for 20 min, supernatants were filtered through sterile 0.2-µm, HT Tuffryn® membrane Acrodisc® syringe filters (Gelman Laboratory, Ann Arbor, MI) and stored in aliquots at −70 °C until use. A total of 10^6 cysts was suspended in 100 µl of the filter-sterilized digestive fluid and incubated for 1 h at room temperature. Then, suspensions were placed on ice for 10 min followed by centrifugation at 2,000 *g* for 10 min at 4 °C. After suspension of the pellets in sterilized water, the dehisced cyst suspensions were layered on top of aqueous Ludox HS-40 step gradients (20%, 40%, 50%, 60%, 70%, and 80%, 1 ml each) and centrifuged at 1,400 *g* for 30 min. Filamentous cells, localized at the interface between 60% and 70% at a density of 1.20 g/ml, were collected, diluted with 5 vol. of sterilized water, and centrifuged at 700 *g* for 10 min. After 3 additional washing cycles, the final pellets were resuspended in sterilized water. Filamentous cells were counted with a hemocytometer and used for experiments.

In vitro production of *Helicosporidium* vegetative cells. In order to produce cyst-free samples of vegetative cells, in vivo-produced cysts were administered by pipette-tip feeding to *S. exigua* or *H. zea* larvae. Hemolymph samples were withdrawn 4 d after the treatment, when vegetative cell development but no cyst formation was observed. Samples were collected into anticoagulant buffer (98 mM NaOH, 186 mM NaCl, 1.7 mM EDTA, 41 mM citric acid, pH 4.5) (Mead, Ratcliffe, and Renwrantz 1986) and centrifuged at 1,000 *g* for 10 min at 4 °C. Pellets were resuspended in anticoagulant buffer. Of these suspensions, 5 µl were inoculated into 500 µl of Hinks'-modified Grace's insect medium (TNM-FH) (Sigma) supplemented with 5% fetal calf serum (FCS) and 50 µg/ml gentamycin in a 24-well format. After 12 d incubation at 26 °C, vegetative cells were harvested, centrifuged, and resuspended in sterilized water. Cells were counted using a hemocytometer and stored at 4 °C until use.

Fluorescent microscopy. To document nuclear division during filamentous cell transformation, filamentous cell preparations were obtained as described above and suspended in 1 ml of liquid medium (TNM-FH+5% FCS+50 µg/ml gentamycin). Aliquots were transferred into a 24-well culture dish and incubated at 26 °C. At different time intervals after incubation, cells were harvested and fixed in acetone for 10 min. Fixed cells were rehydrated in phosphate-buffered saline (PBS), permeabilized for 10 min in 0.4% (v/v) Triton-X 100 in PBS, washed several times in PBS, and then stained with Sytox® Green nucleic acid stain (Molecular Probes, Eugene, OR) following instructions of the manufacturer.

To examine autosporulation during vegetative cell replication of *Helicosporidium*, in vitro-produced vegetative cells were harvested at 3 and 5 d after inoculation during exponential replication. Cells were washed in PBS, fixed in acetone for 10 min, equilibrated in PBS for 5 min, and permeabilized for 10 min in 0.4% (v/v) Triton X-100 in PBS. After several washes in PBS, cells were stained for 30 min in Calcoflour White MR2 (Polysciences, Warrington, PA) (1 mg/ml PBS). Following several washes in PBS, cells were counter-stained with Sytox® Green nucleic acid stain as described above. Stained cells were then suspended in 1,4-diazobicyclo[2.2.2]octane in glycerol (DABCO) antiquenching mounting medium (Sigma) and examined and photographed using differential interference contrast (DIC) or phase contrast and epifluorescence microscopy. Numbers of daughter cells per mother cell were recorded from 100 randomly chosen cells per replicate preparation (n = 3). Cell diameters were measured using SPOT Advanced software (Diagnostic Instruments Inc., Sterling Heights, MI).

Transmission electron microscopy (TEM). For TEM examination, pellets of in vitro-produced filamentous cells or vegetative cells or in vivo-produced cysts were fixed for 2 h in 2.5% (v/v) glutaraldehyde (EM grade) and 1% (v/v) acrolein solution in 0.1 M cacodylate buffer preheated to 60 °C (Glauert 1975). Following fixation, samples were washed 3 times in 0.1 M cacodylate buffer (pH 7.2) and post-fixed in 1% (w/v) aqueous osmium tetroxide for 1 h at room temperature. Samples were washed 3 times with distilled water and pellets were embedded in 3% aqueous agar for easier handling. They were then dehydrated through a standard ethanol series (30–100% ethanol, 15 min per step) and cleared with 2 washes in acetone. Samples were infiltrated with Epon-Araldite resin in a stepwise fashion with ratios of acetone to resin of 3:1, 1:1, and 1:3, and finally several changes of pure resin (Glauert 1975). Resin blocks were cured overnight in a 65 °C oven. Thin gold interference sections (85–100 nm thick) were collected on 200-mesh nickel grids and stained in uranyl acetate and lead citrate. Sections were observed and photographed at 75 kV in a Hitachi H-600 transmission electron microscope.

Filamentous cell transformation. For light microscopic observations, filamentous cell preparations were produced as described above, and diluted as necessary to obtain a concentration of 20–25 filamentous cells per microliter. One-microliter droplets were applied to sterilized glass slides coated with thin layers of TNM-FH+5% FCS+50 µg/ml gentamycin containing 1% agarose. Eight slides, each with 3–4 inoculations, were prepared. These micro-cultures were transferred to sterile agar Petri dishes, sealed with parafilm, and incubated at 26 °C. Over a 4-day period, individual filamentous cells (n = 10 per slide) were identified via recorded *x–y*-coordinates and photographed at 24-h intervals under light microscopic optics with phase contrast and DIC. Measurements of filamentous cell length, diameter at the slender and swollen ends, and average daughter cell area were computed from photographs using SPOT Advanced software. In addition, ratios of ruptured to intact filamentous cells and numbers of daughter cells produced per filamentous cell were determined daily.

Vegetative cell colonies originating from individual filamentous cells were inoculated into liquid medium (TNM-FH+5% FCS+50 µg/ml gentamycin) and a series of 96 clones was produced. After a 7-day incubation at 26 °C, 12 randomly selected clonal vegetative cell preparations were harvested, centrifuged at 2,000 *g* for 10 min, resuspended in sterilized water, and counted using a hemocytometer. Cell concentration was adjusted to 10,000 cells/µl. Five microliters of each sample were transferred to medium (in vitro transfer) and incubated at 26 °C. Another 5 µl were injected into the hemocoels of *S. exigua* larvae (n = 5 per sample) (in vivo transfer). Larvae were incubated at constant conditions (26 °C ± 1 °C, 70% ± 5% RH, 12-h photoperiod) and provided with diet ad libitum. Hemolymph examinations were conducted 7 d after injection. The presence/absence of cysts was recorded for both the in vitro and in vivo transfers after 7 d.

Replication dynamics of vegetative cells in vivo and in vitro. Vegetative cells were produced in vitro as described above and diluted in sterilized water to a final concentration of 1,000 cells/µl. To observe in vitro multiplication of vegetative cells, 5,000 vegetative cells were inoculated into 500 µl TNM-FH+5% FCS+50 µg/ml gentamycin and incubated at 26 °C. After different time intervals, cells were harvested, centrifuged, resuspended in 50 or 500 µl of sterilized water, and counted using a hemocytometer. Dilutions were made as necessary. Five replicate assays with triplicate readings (harvests) at different time points were conducted.

In an additional experiment, the effect of media depletion on vegetative cell multiplication was examined: cells were harvested after 12 d as described above and the cell-free supernatant (depleted medium) was saved for re-inoculation. A total 5,000 vegetative cells was then inoculated into the corresponding depleted medium and into fresh medium (first transfer experiment). After 12 d, cells were harvested, counted, and 5,000 cells

produced in depleted medium were again inoculated into the corresponding depleted and into fresh medium (second transfer experiment). Three replicate assays with duplicate or triplicate cultures were conducted per transfer experiment.

The in vivo replication dynamics were investigated in 2 different noctuid hosts. Fifth instar larvae of *S. exigua* and *H. zea* were injected with 5,000 in vitro-produced vegetative cells per larva. In the experiment with *S. exigua*, larvae were also injected with 50,000 vegetative cells per larva. In the experiment with *H. zea*, control insects were injected with sterilized water. Insects were incubated at constant conditions (26 °C ± 1 °C, 70% ± 5% RH, 12-h photoperiod) and provided with diet ad libitum. Over a time period of 8 d after the treatment, hemolymph samples were withdrawn daily for cell counts. The pH of undiluted hemolymph was measured using pH test strips (Sigma). For cell counts, 5 µl of hemolymph were collected into 45 µl anticoagulant buffer and visualized under DIC light microscopic optics to record the presence of vegetative cells, cysts, and hemocytes. If necessary, suspensions were diluted in Ringer's physiological solution (0.75% NaCl, 0.035% KCl, 0.021% $CaCl_2$), and vegetative cells and cysts were counted using a hemocytometer. In the experiment with *H. zea*, numbers of hemocytes were also determined. In an additional assay, larvae of *H. zea* were examined at 10, 12, and 14 d after injection in order to record helicosporidial development after the host's death (10–12 d after injection). For all experiments, cell numbers were calculated as cells per microliter of hemolymph and the percentage of cysts was determined as number of cysts per total number of helicosporidial cells. Each experiment was replicated 3 times with 2 or 3 replicate insects per time interval.

Statistics. Statistical analyses were conducted using the SAS System for Windows (SAS 1999). Filamentous cell lengths, widths of individual filamentous cells at their anterior and posterior end measured 24 h after inoculation, and initial and final cell numbers were subjected to *t*-test comparisons (proc ttest) (Köhler, Schachtel, and Voleske 1992). The area size of daughter cells at different time intervals and cell numbers produced per microliter of medium or hemolymph were evaluated by analysis of variance using the SAS procedure for general linear models (proc glm) in balanced designs or the procedure for mixed linear models (proc mixed) in unbalanced designs; means were separated using the SAS least square means statement (lsmeans) (Rao 1998; Younger 1998). Cell frequency patterns during autosporulation were compared by logistic regression using the SAS genmod procedure (proc genmod) and the lsmeans statement (Neter, Wasserman, and Kutner 1990). Cell volumes were computed from cell diameters and then subjected to analysis of variance (proc glm and lsmeans statement) (Rao 1998; Younger 1998). Unless stated otherwise, means are accompanied by the standard error (SE).

RESULTS

Cysts and filamentous cells. The cyst, which is the characteristic life stage of *Helicosporidium*, is composed of a pellicle containing 3 ovoid cells and 1 elongate filamentous cell, which coils 3 to 4 times along the perimeter of the cyst (Fig. 1) (Boucias et al. 2001). The pellicle was thicker in the lateral regions (75–93 nm, n = 10) compared with the dorsal/ventral regions (50–53 nm, n = 10) (Fig. 2). A single membrane surrounded each of the ovoid cells (Boucias et al. 2001) (Fig. 1), and lipid deposits within the dense cytoplasm were characteristic for these cyst-contained cells (Fig. 1).

Incubation of cyst preparations in digestive fluids harvested from noctuid host larvae stimulated the dehiscence of the cysts and resulted in the release of ovoid and filamentous cells (Fig. 2, 3). The rupture of the cyst pellicle occurred along a fracture line in the ventral/dorsal region, where the pellicle was thinner than in the lateral regions (Fig. 2). Following the release, the ovoid cells deteriorated (Fig. 2). The filamentous cell was surrounded

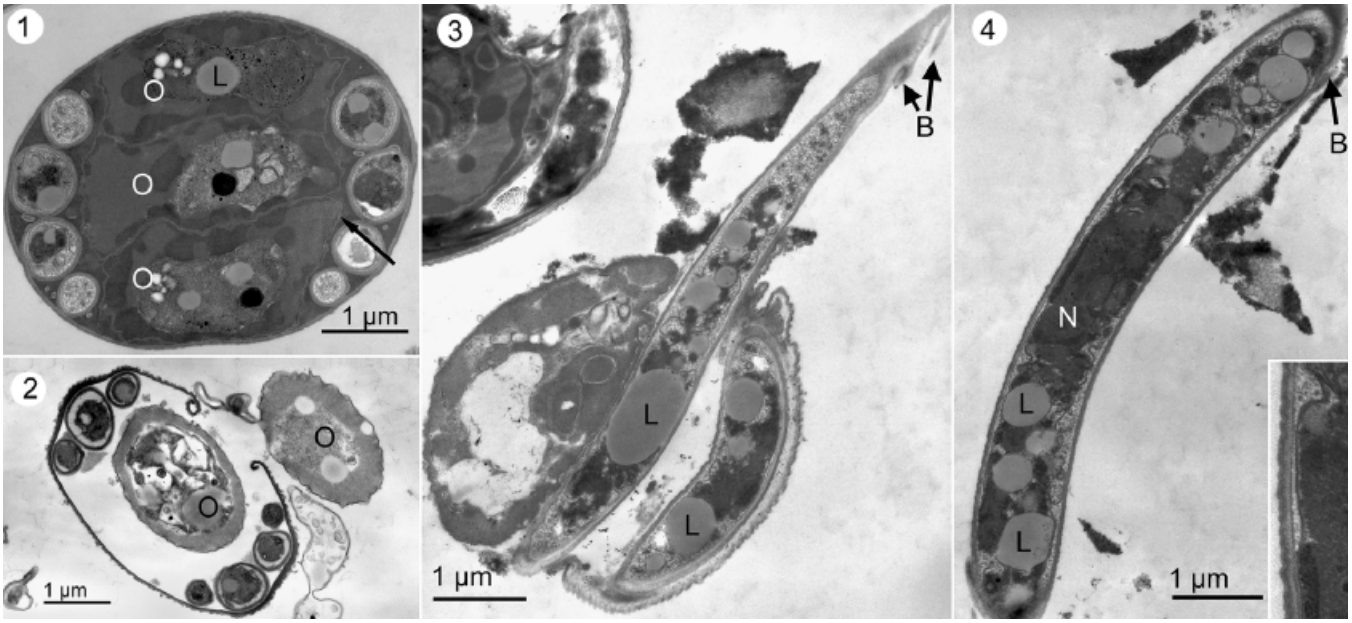

Fig. **1–4.** Transmission electron micrographs documenting the release of the filamentous cell from the cyst stage of isolate SjHe of *Helicosporidium*. Scale bars = 1 µm. **1.** Cyst isolated from the black fly, *Simulium jonesi*. Note the lipid deposits (L) characteristic for ovoid cells (O) and filamentous cells inside the cysts. **2.** Dehiscing cyst: deteriorated ovoid cell (O) is released through a ruptured pellicle while the filamentous cell is coiled inside. Note that the cyst ruptures in ventral/dorsal regions, where the pellicle is thinner. **3.** Release of the filamentous cell, the surface of which is covered by characteristic barbs (B). Note the abundant lipid deposits (L) inside the cell. **4.** Portion of a released filamentous cell. Note the nucleus (N), the barb (B), the abundant lipid deposits (L), and a dense appearance of the cytoplasm characteristic for cysts-contained and newly released filamentous cells. The inset shows a magnification of the filamentous cell pellicle composed of multiple layers.

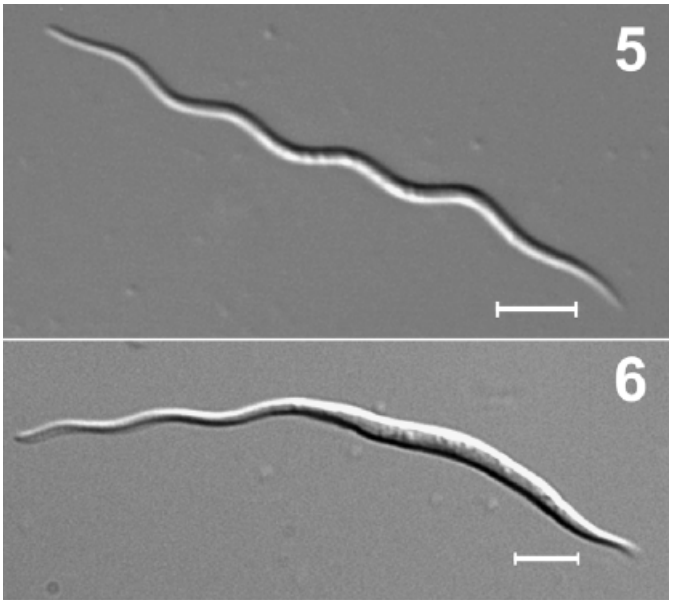

Fig. **5–6.** Initial filamentous cell transformation of isolate SjHe of *Helicosporidium* under controlled in vitro conditions. Scale bars = 5 μm. **5.** Purified filamentous cell at the time of inoculation. **6.** Partial swelling of the filamentous cell observed within 24 h after inoculation.

by a multilaminate pellicle, which was, in contrast to the cyst pellicle, composed of at least 3 layers (Fig. 4, inset) and coated with characteristic surface projections or barbs (Boucias et al. 2001) (Fig. 3). Total thickness of the filamentous cell pellicle of cyst-contained and newly released filamentous cells measured 35–53 nm (n = 10). Newly released filamentous cells were uninucleate and contained in a dense cytoplasm abundant lipid deposits, which were also characteristic for cyst-contained ovoid cells (Fig. 1, 3, 4).

Filamentous cell transformation. Owing to suboptimal growth conditions provided by inoculation of single filamentous cells onto solid medium, the timing of the different events during filamentous cell transformation may be considered as estimations. The transformation process was initiated by a swelling of one end of the filamentous cells along with a reduction in length (Fig. 5, 6). Within 24 h after inoculation, the widths of individual filamentous cells differed significantly between the slender (0.9 ± 0.03 μm, n = 20) and the swollen end (1.4 ± 0.03 μm, n = 20) ($P < 0.0001$, $t = 13.71$, df = 19, proc ttest). In this phase of transformation, filamentous cells were 39 ± 1 μm (n = 20) long and significantly shorter than filamentous cells that were measured immediately after dehiscence (53 ± 2 μm, n = 10) ($P < 0.0001$, $t = 10.08$, df = 28; proc mixed and lsmeans).

Ultrastructural examination and fluorescent staining revealed the migration of the cytoplasm and nucleus to the swollen portion of the filamentous cell (Fig. 7, 8) followed by 2 nuclear divisions (Fig. 9–14). Transforming filamentous cells were characterized by the absence of lipid droplets, and a less dense appearance of the cytoplasm (Fig. 8) as well as a thinner pellicle (20–26 nm, n = 10) when compared with cyst-contained and newly released filamentous cells. Nuclear division was followed by cytoplasmic division (Fig. 9–10). Subsequently, a layer of new pellicle material (6–10 nm thick, n = 10) was deposited around the daughter cells resulting in 2 pellicle layers, an old layer with barbs and new layer without barbs (Fig. 10).

At 48 h, 79% ± 4% (n = 40) of the observed filamentous cells ruptured along the horizontal axis of the pellicle and released 4 elongate, rod-shaped daughter cells (Fig. 15, 16). The enclosing pellicle of these cells was 12–18 nm thick (n = 10). The quartet of elongate daughter cells then divided into 8 oval to spherical vegetative cells that underwent further replication (Fig. 17). At 96 h, almost all filamentous cells (96% ± 3%, n = 80) had ruptured and many had produced clones containing up to 32 vegetative cells (Fig. 18). Twelve randomly selected clonal vegetative cell preparations derived from transformed filamentous cell were used for parallel in vitro and in vivo transfers. These vegetative cells did not differentiate into cysts under in vitro conditions (n = 12) (Fig. 19). However, within 7 d after injection into the hemocoels of *S. exigua* larvae, cyst formation was observed in 100% of the insects (n = 60) (Fig. 20). Using DIC light microscopic optics, central ovoid cells and/or the coiled, peripheral filamentous cell could be observed in the cysts (Fig. 20), in contrast to a uniform, granular cytoplasm seen in the vegetative cells (Fig. 19, 20).

Autosporulation process. The in vitro replication of *Helicosporidium* was characterized by the production of vegetative cells that underwent autosporogenic division. Replicating vegetative cells produced 2, 4, or 8 cells per mother cell (Fig. 21). Vegetative cells contained mitochondria, Golgi apparatus, a single nucleus, and dark granules in the cytoplasm, which were not identified but resemble starch granules (Fig. 22–30). The presence of elongate mitochondria was characteristic for single-cell vegetative stages (Fig. 22, 25). As described during filamentous cell transformation, nuclear and cytoplasmic divisions and the formation of daughter cell pellicles occurred within the pellicle of the mother cell (Fig. 26, 28, 29). Upon maturation, the daughter cells were released (Fig. 27, 30) and underwent additional cycles of vegetative replication. Rupture of the old pellicle and release of the daughter cells was observed in 2-, 4-, and 8-cell stages (data not shown). A significant portion of single vegetative cells secreted new pellicle material without undergoing a cell division (Fig. 23) followed by the shedding of the old pellicle (Fig. 24). Both old and newly formed pellicles were equally thick (30–35 nm, n = 10, and 25–35 nm, n = 10, respectively).

Daughter cell counts conducted during the exponential phase of vegetative cell replication (3 and 5 d after inoculation) revealed that 46% ± 5% (n = 6) of the vegetative cell population were single-cell stages, whereas 24% ± 2%, 23% ± 3%, and 8% ± 1% (n = 6) contained 2, 4, and 8 daughter cells within the pellicle of the mother cell, respectively. The frequency pattern did not change over time during exponential replication (between 3 and 5 wk after inoculation) ($P > 0.05$, $\chi^2 \leq 3.41$, df = 1, proc genmod). After vegetative cell cultures had reached the stationary phase, significantly higher numbers of single-cell stages were recorded (70% ± 4%) ($P < 0.0001$, $\chi^2 = 15.48$, df = 1, proc genmod). The frequency of 2-cell stages decreased significantly to 10% ± 2% ($P = 0.0050$, $\chi^2 = 7.88$, df = 1, proc genmod), whereas frequencies of 4-cell stages (14% ± 2%) and 8-cell stages (7% ± 0.3%) were not significantly different from the frequencies found during the exponential phase ($P = 0.0835$, $\chi^2 = 3.00$ and $P = 0.8756$, $\chi^2 = 0.02$, respectively, df = 1, proc genmod).

Comparison of the cell volumes between vegetative cells containing 1, 2, 4, or 8 daughter cells showed an approximate doubling of the cell volume from an average of 21.6 to 44.3 μm^3 before cell division occurred (Table 1). The minimum cell volume of single-cell stages was 8.2 μm^3. During maturation the volume of these cells reached a maximum of 44.6 μm^3, thereby approaching the average cell volume of the 2-cell stage (44.3 μm^3). A similar scenario of cell volume increase before daughter cell division was observed during the transition from 2-cell to 4-cell and from 4-cell to 8-cell stages (Table 1).

In vitro replication dynamics of vegetative cells. Cell numbers produced in vitro were counted over a time period of 14 d. Beginning with 10 cells per microliter in 500-μl cultures, replication dynamics showed a sigmoid progression with an initial

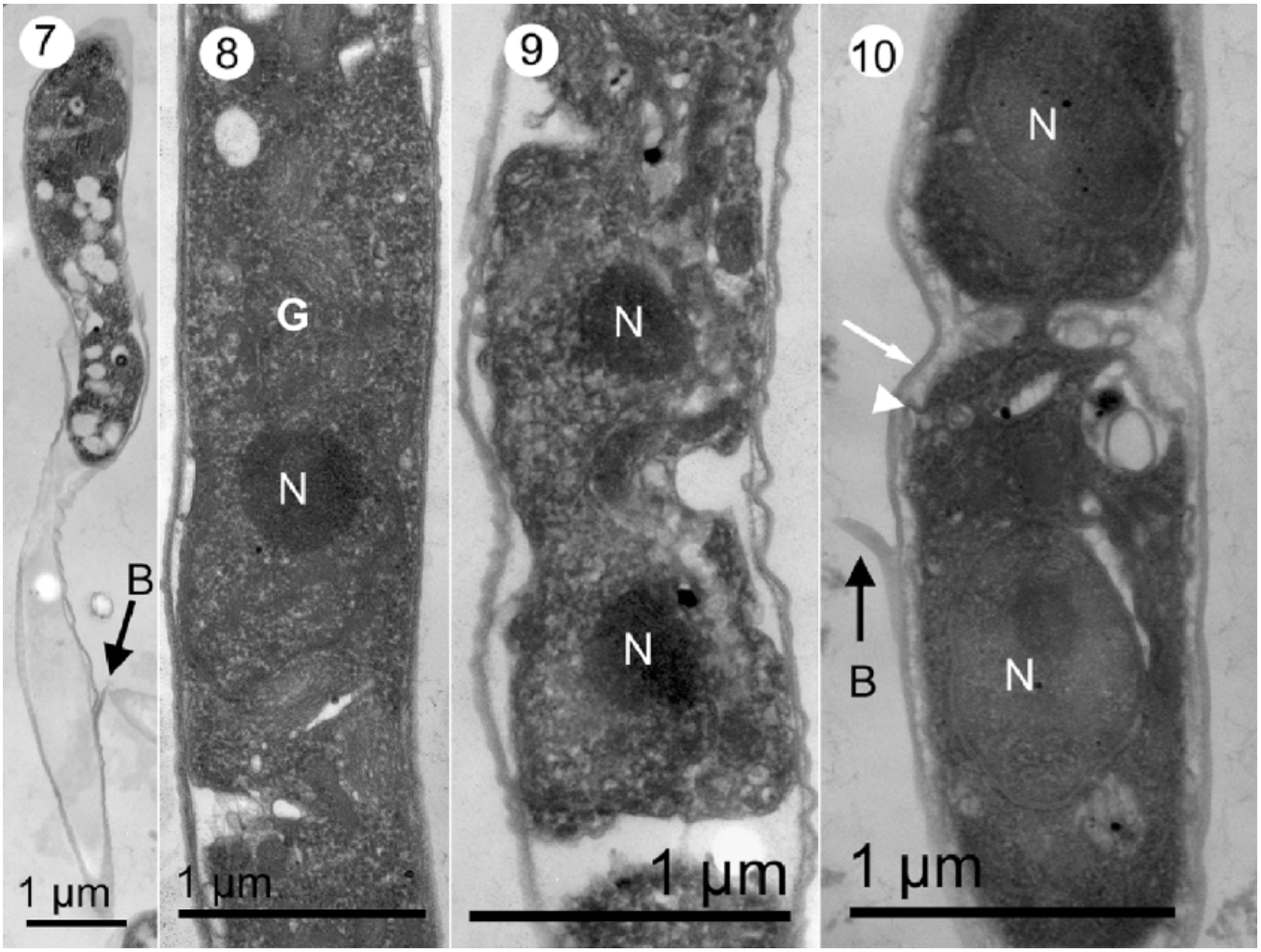

Fig. **7–10.** Transmission electron micrographs documenting nuclear and cytoplasmic division during filamentous cell transformation of isolate SjHe of *Helicosporidium*. Scale bars = 1 µm. **7.** Initial migration of the cytoplasm into one portion of the cell and emptying of the rest of the filamentous cell. Note the barb (B) on the pellicle of the empty region. **8.** Portion of a transforming filamentous cell showing the nucleus (N) and Golgi apparatus (G). Note the absence of the lipid deposit droplets and a less dense appearance of the cytoplasm than in cyst-contained and newly released filamentous cells. **9.** Nuclear and cytoplasmic division in a transforming filamentous cell. Note that the cytoplasmic division occurs within the old pellicle before the pellicle formation around the progeny cells. **10.** Dividing progeny cells formed within the old barb-containing (B) pellicle (white arrow) of the transforming filamentous cell. Note the formation of the new pellicle (white arrowhead) around the progeny cells and a bridge of cytoplasm still connecting the cells.

lag phase of 1.5 d and a log phase between 1.5 and 6 d (Fig. 31). Doubling time during this phase (4.5 d) of exponential replication was 8 h. Within 7 d, vegetative cells reached the stationary phase with a density of $1.27 \pm 0.04 \times 10^5$ cells/µl medium (n = 54). No cyst differentiation occurred in these in vitro cultures.

Table **1.** Volumes of SjHe *Helicosporidium* vegetative cells containing one, two, four, and eight daughter cells per mother cell.

Cell stage	N	Cell volume of the mother cell (µm^3)		
		Mean ± SE	Minimum	Maximum
Single	484	21.6 ± 0.3	8.2	44.6
Two	174	44.3 ± 0.6	26.5	63.5
Four	177	66.0 ± 0.8	36.1	94.4
Eight	65	92.0 ± 2.4	59.7	175.8

Cells were grown at 26 °C in TNM-FH broth supplemented with 5% FCS and 50 µg/ml gentamycin.

Transfer experiments showed a significant inhibition of cell multiplication in depleted medium (first transfer: $P < 0.0001$, $t = -13.19$, df = 68, second transfer: $P < 0.0001$, $t = -14.30$, df = 68, proc mixed). Within 12 d after the first transfer, numbers of vegetative cells produced in fresh medium ($1.39 \pm 0.07 \times 10^5$, n = 18) exceeded cell numbers produced in depleted medium ($1.34 \pm 0.50 \times 10^4$, n = 18) by 55-fold. Within 12 d after the second transfer, numbers of vegetative cell produced in fresh medium ($1.38 \pm 0.11 \times 10^5$, n = 18) exceeded cell numbers produced in depleted medium ($1.38 \pm 0.27 \times 10^3$, n = 33) by 331-fold. Owing to high variations between replicate cultures, the additional suppression of cell replication after a second transfer into depleted medium was not significant when compared with suppression after the first transfer into depleted medium ($P = 0.2124$, $t = 1.26$, df = 68, proc mixed). After multiple transfers into fresh medium, vegetative cell cultures were characterized by the formation of non-motile adherent cells that clustered together via production of extracellular mucilage, resulting in a palmelloid cell phenotype (Fig. 32).

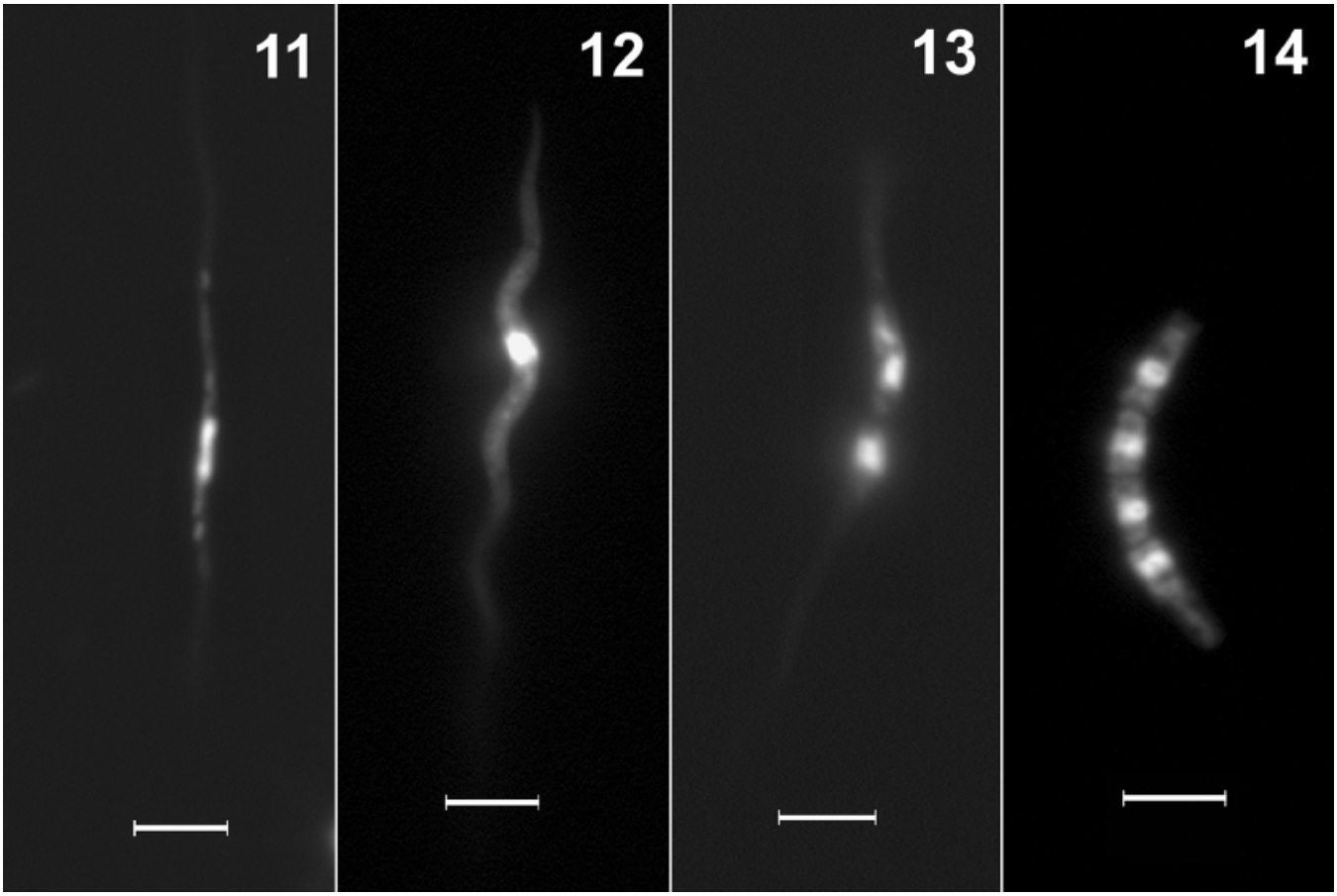

Fig. **11–14.** Nuclear division during the transformation process of filamentous cells of isolate SjHe of *Helicosporidium*. Cells were fixed and permeabilized in acetone/Triton X-100 and stained with Sytox® Green nucleic acid stain. Scale bars = 5 μm. **11.** Diffuse distribution of nuclear material at the time of inoculation. **12.** Concentration of nuclear material in the thickening portion of the filamentous cell 24 h after inoculation. **13.** Three nuclei seen after 48 h. **14.** Four distinct nuclei and cytoplasmic division observed after 72 h.

In an attempt to identify factors responsible for cyst morphogenesis, 2 additional experiments examined the effect of either high cell density or media exchange on *Helicosporidium* development in vegetative cell cultures. The inoculation of $1.27 \pm 0.09 \times 10^6$ vegetative cells/μl medium (n = 3) into 500-μl cultures did not result in cyst formation within 12 d, and the cell density remained at $1.37 \pm 0.10 \times 10^6$ cells/μl ($P = 0.5400$, $t = -0.73$, df = 2, proc ttest). The exchange of medium in stationary-phase cultures at a cell concentration of $1.27 \pm 0.04 \times 10^5$ cells/μl medium (Fig. 31) resulted in additional cell multiplication yielding twice as many vegetative cells per microliter of medium ($2.46 \pm 0.11 \times 10^5$ cells/μl, n = 9). However, no cyst formation occurred within 12 d after the media exchange.

In vivo development of *Helicosporidium*. Infected and control larvae of both *S. exigua* and *H. zea* underwent metamorphosis and formed prepupae and pupae. The pH of hemolymph samples ranged between 6.3 and 6.5.

In the experiment with *S. exigua*, larvae were injected with 2 different dosages of *Helicosporidium* vegetative cells (5,000 and 50,000 cells per larva). Statistical analysis showed no significant difference in cell numbers between the 2 dosages tested ($P = 0.0730$, $F = 3.28$, df = 102, proc mixed): mean numbers of helicosporidia per microliter of hemolymph increased from 2.76×10^3 cells recorded 1 d after injection to 1.97×10^6 cells recorded after 8 d (Table 2). Doubling time during the exponential phase (3 d) of vegetative cell replication was 7 h. Regardless of the initial dosage, cyst morphogenesis was first observed in 33% of the insects after 4 d (Table 2). At this time, average cell density was 6.99×10^5 cells/μl (Table 2). After 5 d, cysts were formed in 75% of the insects when average cell densities were at 9.09×10^5 cells/μl (Table 2). After 6 and 8 d, cysts were seen in all insects and average cell densities were 1.68×10^6 and 1.97×10^6 cells/μl (Table 2), respectively. The proportion of cysts determined in insects with cyst formation increased from 4% at 4 d to 21% at 8 d (Table 2).

In parallel experiments with *H. zea*, mean numbers of helicosporidia produced per microliter of hemolymph increased from 411 cells after 1 d to 6.00×10^6 cells after 8 d (Table 2). The stationary phase in this host was reached after 5 d (Table 2). Doubling time during the exponential phase (4 d) of vegetative cell replication was 7 h. Cyst morphogenesis was first observed in 67% of the insects after 5 d, in 89% after 6 d, and in all insects after 8 d (Table 2). The proportion of cysts determined in insects with cyst formation increased from 6% at 5 d to 15% at 8 d (Table 2). Hemocyte numbers did not differ between *Helicosporidium*-infected and control insects and did not change within a time frame of 8 d after injection, that is during the development from 5th instar larvae to pupae ($P = 0.6967$, $F = 0.64$, df = 98, proc mixed). Mean numbers of hemocytes per microliter of hemolymph were $1.43 \pm 0.04 \times 10^4$ (n = 112).

In an additional assay, helicosporidial cell numbers and cyst formation were also recorded in *H. zea* at 10, 12, and 14 d after

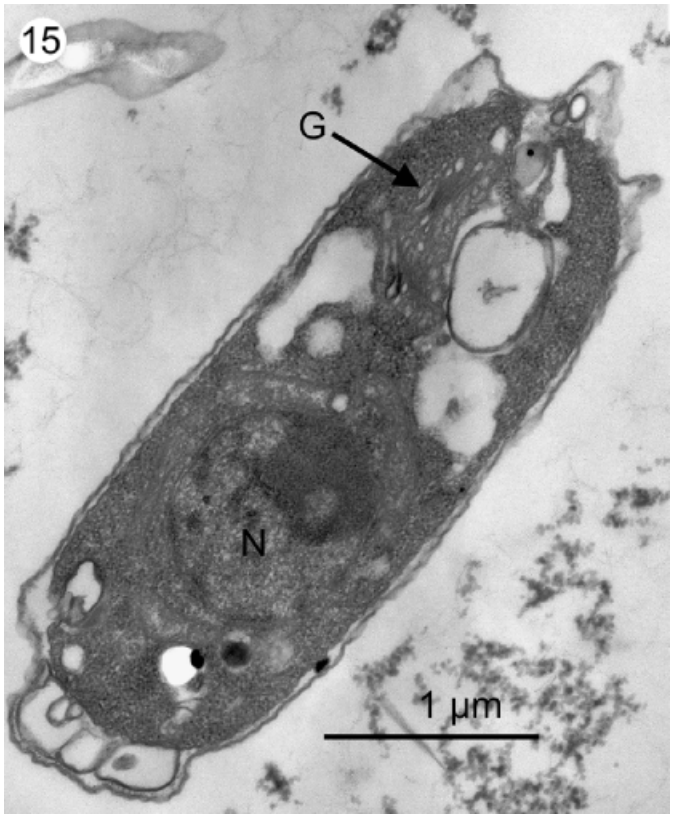

Fig. **15.** Newly formed elongated progeny cell released from the ruptured pellicle of a filamentous cell. Note the nucleus (N), Golgi (G) and the new pellicle.

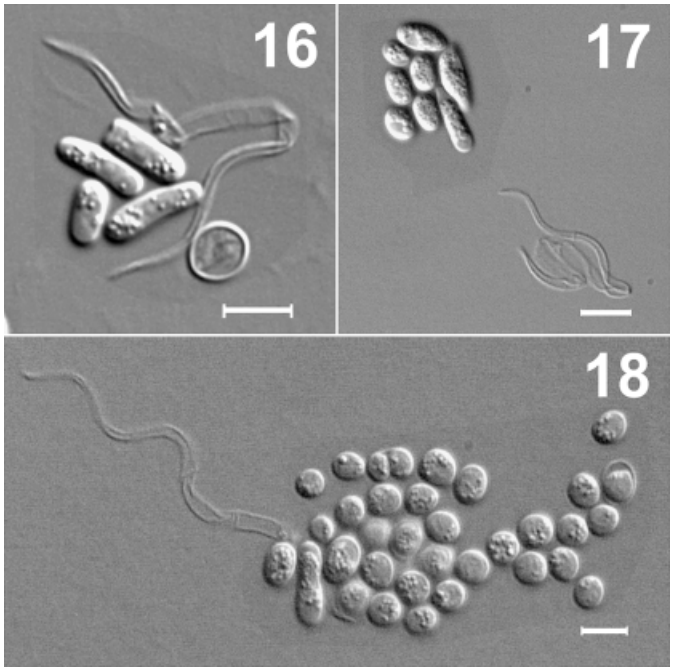

Fig. **16–18.** Late transformation phase of filamentous cells into vegetative cells of isolate SjHe of *Helicosporidium* under controlled in vitro conditions. Scale bars = 5 µm. **16.** Ruptured filamentous cell releasing 4 rod-shaped progeny cells after 48 h. **17.** Filamentous cell pellicle and 8 oval to spherical vegetative cells at 72 h. **18.** Clone of 32 vegetative cells originating from a filamentous cell after 96 h.

injection and data were included in the statistical analysis. All insects were dead on day 12 after the treatment. Numbers of helicosporidia per microliter of hemolymph after 10 d (6.78×10^6) were not significantly different from numbers recorded after 5, 6, and 8 d (Table 2). Postmortems at 12 and 14 d showed a significant increase in cell numbers with a mean of 9.62×10^6 cells per microliter of hemolymph ($P \leq 0.0075$, $t \leq -2.74$, df = 80, proc mixed). Cysts were produced in all insects examined after 10, 12, and 14 d (n = 27). The proportion of cysts stayed constant at 17 ± 2% (n = 18) between 10 and 12 d ($P = 0.1258$, $t = -1.55$, df = 80, proc mixed) and decreased significantly to 11 ± 2% (n = 9) at 14 d ($P = 0.0014$, $t = 3.31$, df = 80, proc mixed) (Table 2). Cyst differentiation did not increase as a response to death of the insect host.

DISCUSSION

Helicosporidium sp. has recently been identified as an achlorophyllous, entomopathogenic alga within the Class Trebouxiophyceae (Chlorophyta) (de Koning and Keeling 2004; de Koning et al. 2005; Tartar and Boucias 2004). This organism has retained a functional plastid genome (Tartar and Boucias 2004), which has recently been sequenced (de Koning, pers. commun.). In addition, the identification of nucleus-encoded genes for plastid-targeted proteins in *Helicosporidium* sp. has demonstrated the presence of cryptic plastids, which are highly derived non-photosynthetic cell organelles (de Koning and Keeling 2004). Cryptic plastids and their genomes have been reported in a variety of non-photosynthetic protists, including the chlorophyte *Prototheca wickerhamii* (Borza, Popescu, and Lee 2005; Knauf and Hachtel 2002), the euglenoid *Astasia longa* (Gockel and Hachtel 2000), and the apicomplexan parasites *Plasmodium falciparum* and *Toxoplasma gondii* (Wilson 2005). While cryptic plastids can be recognized by investigations of their metabolism and genome, the lack thylakoid structures and pigments makes them difficult to detect using microscopic techniques. In fact, these organelles have not been identified in ultra-thin sections of *Helicosporidium* sp. Recently, in an ultrastructural study on a newly discovered bark beetle isolate of *Helicosporidium* sp., Yaman and Radek (2005) pointed out that inclusions described in different cell phenotypes closely resemble a pyrenoid of a chloroplast with associated starch. Similar inclusions could be seen in our ultra-thin sections, but their chemistry could not be identified with the methods used herein.

Helicosporidium sp. is characterized by a unique cyst stage, which ruptures in the midgut lumen of the host and releases an invasive filamentous cell. This mechanism of expelling an invasive life stage into the host appears different from strategies utilized by other animal pathogens. Infective spores of several obligate intracellular parasites contain specialized extrusive organelles to mediate the injection of parasite cytoplasm into the host cell (Beakes and Glockling 1998). Microsporidia, for example, produce spores containing a long coiled polar filament that, upon activation in a suitable host, extrudes from the spore to become a hollow tube and penetrates the membrane of a new host cell, thus facilitating inoculation of the infective sporoplasm into the host cell (Franzen et al. 2005). Microsporidial filament eversion is a result of increased osmotic pressure in the spore and subsequent influx of water, potentially regulated by specific transmembrane pathways, the creation of a proton gradient, variation in carbohydrate levels in the sporoplasm, or active Ca^{2+} influx (Bigliardi and Sacchi 2001; Dall 1983; Frixione et al. 1997; Pleshinger and Weidner 1985; Undeen and Vander Meer 1994).

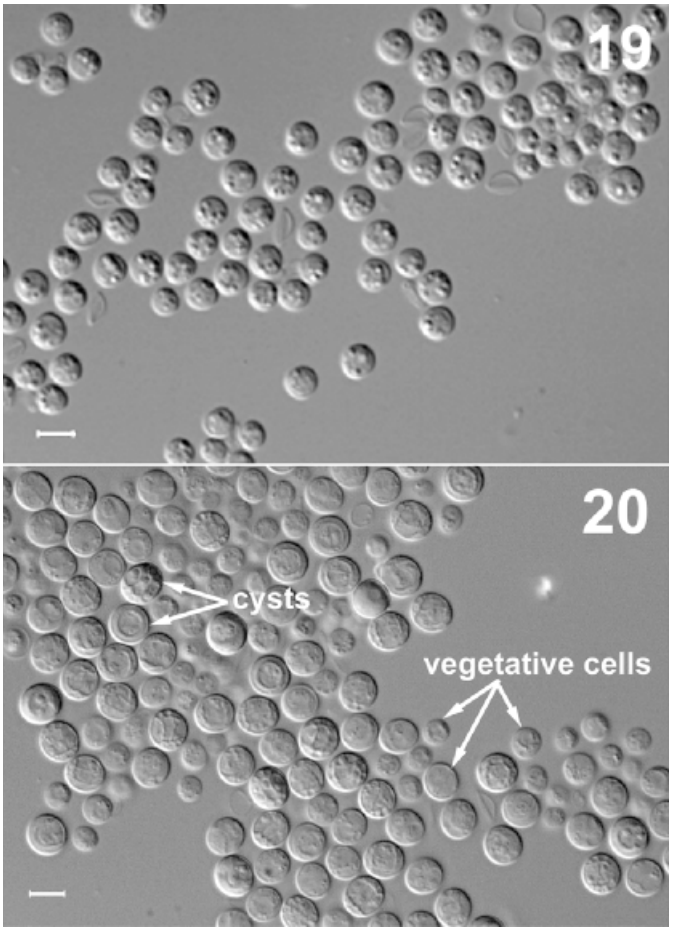

Fig. **19–20.** Development of vegetative cell clones of isolate SjHe of *Helicosporidium* 9 d after in vitro inoculation (**19**) and 7 d after injection into *Spodoptera exigua* larvae (**20**). Note that cyst formation only occurred in the insect. Scale bars = 5 μm.

Nematode-infecting fungi of the biflagellate genus *Haptoglossa* produce highly specialized ''gun'' cells containing a harpoon-shaped projection organelle within a looped, invaginated injection tube; upon discharge and eversion of the tube, the harpoon penetrates the host cuticle and then serves as a hypodermic conduit through which the parasite cytoplasm is injected into the host. Mechanisms other than direct contact with the nematode host or the experimental application of pressure that would trigger the gun cell discharge remain unknown (Beakes and Glockling 1998).

The dehiscence process of *Helicosporidium* cysts can be experimentally induced by enzymatic activity of digestive fluids harvested from susceptible host insects. However, various physical and chemical treatments have failed to stimulate dehiscence (Boucias et al. 2001). Incubation in proteinase K only induces dehiscence after pre-treatment of cysts with a membrane permeability enhancer, dimethyl sulfoxide (DMSO) (Bläske-Lietze, Boucias, and Botts, pers. observ.).

Once released into the midgut lumen of the host, filamentous cells pass through the midgut epithelium and gain ingress into the hemocoel, where the pathogen undergoes multiple cycles of vegetative replication (Bläske-Lietze and Boucias 2005; Boucias et al. 2001). The present in vitro experiments, for the first time, clearly elucidated the transition from the invasive filamentous cell to the replicating stage of *Helicosporidium*, a process that has remained unobserved since the first description of this pathogen by Keilin in 1921 (Yaman and Radek 2005). Each filamentous cell released a quartet of rod-shaped progeny cells, which divided into 8 oval to spherical vegetative cells and then underwent several cycles of cell division. Contrary to other modes of cell division, such as binary fission or budding, the formation of the daughter cell pellicles in both filamentous and vegetative cells of *Helicosporidium* took place within the pellicle of the mother cell. This process of autosporulation has been described in other green microalgae within the class Trebouxiophyceae (Chlorophyta), including *Trebouxia erici* and different species of *Chlorella* (Huss et al. 2002; Yamamoto et al. 2003), *Nannochloris* (Yamamoto et al. 2003), and *Prototheca* (Pore 1985; Poyton and Branton 1972; Wong and Beebee 1994). Whereas in certain species up to 32 daughter cells can be contained within the mother cell (Yamamoto et al. 2003), vegetative cells of

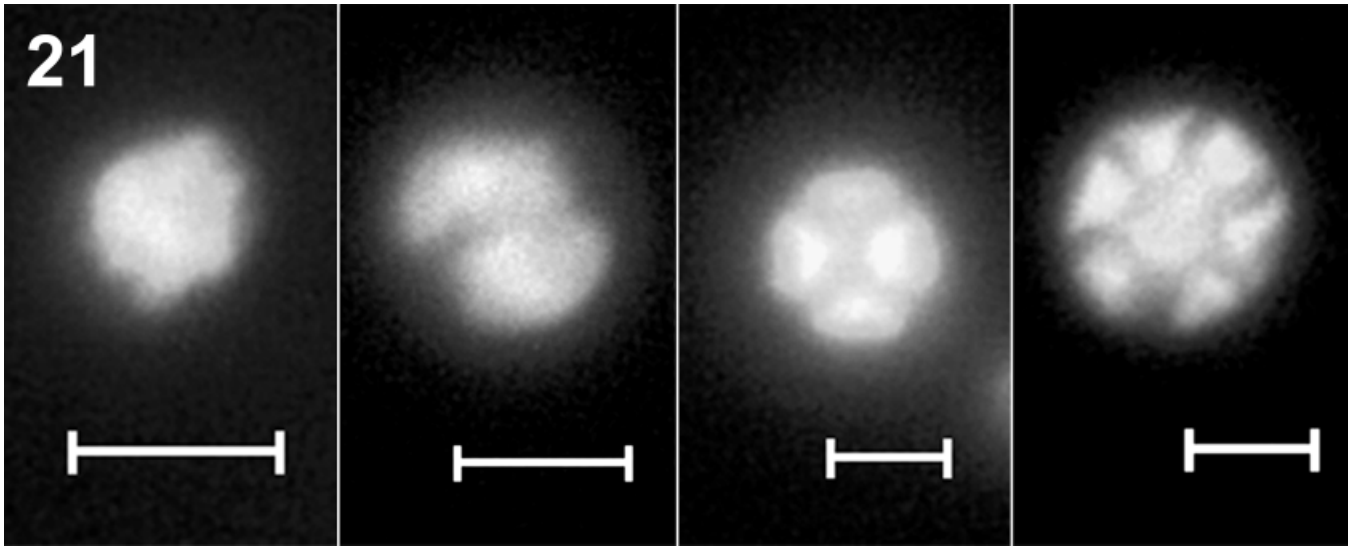

Fig. **21.** Autosporulation during vegetative cell replication of isolate SjHe of *Helicosporidium* showing a sequence of 1, 2, 4, and 8 daughter cells (left to right) within the cell wall of the mother cell. Vegetative cells were fixed and permeabilized in acetone/Triton X-100 and stained with Calcoflour White MR2. Scale bars = 3 μm.

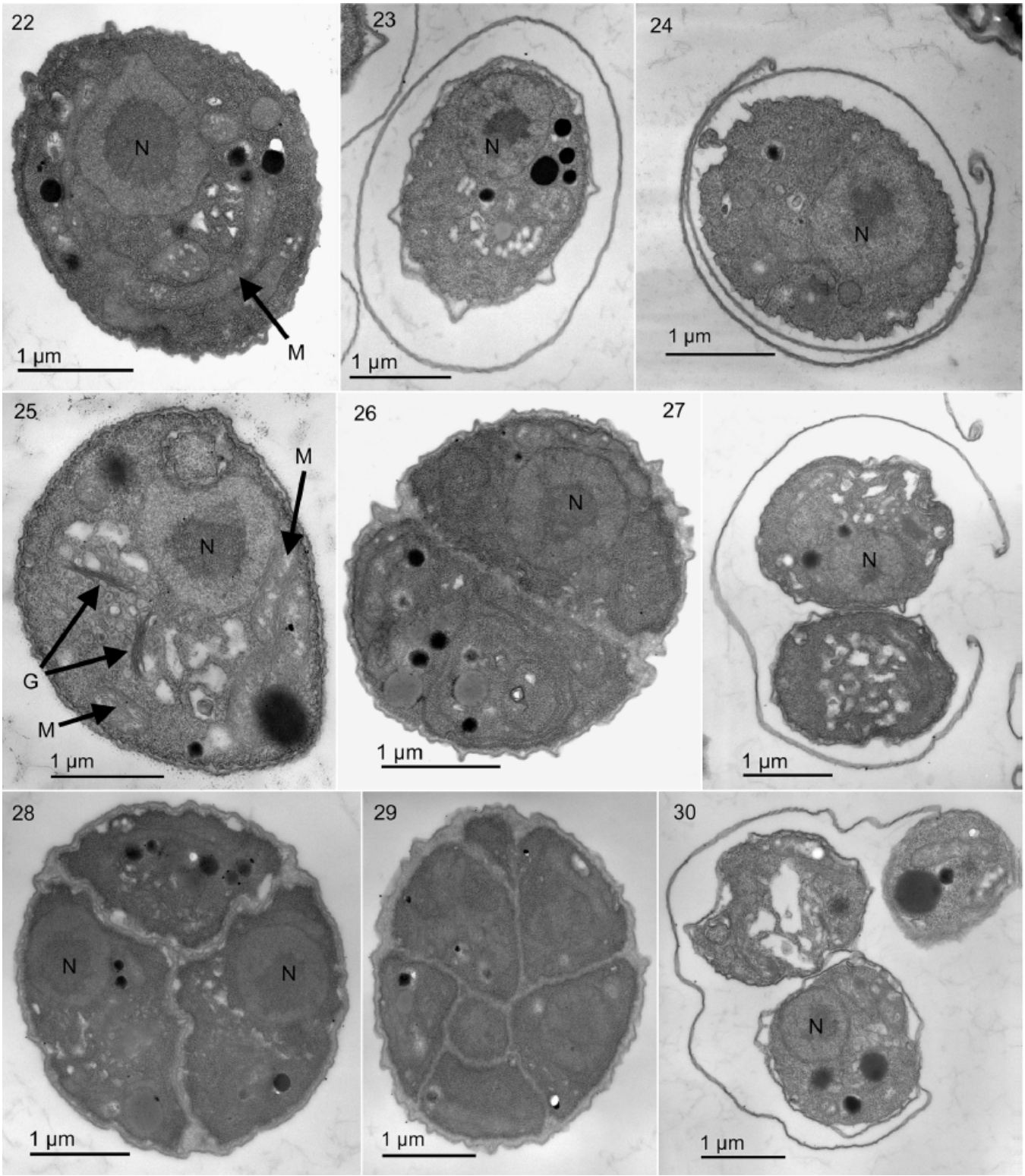

Fig. **22–30.** Transmission electron micrographs of in vitro-produced vegetative cells of isolate SjHe of *Helicosporidium* during different phases of replication. **22–24.** Shedding cycle of 1-cell vegetative stages. **22.** A typical vegetative cell with a characteristic long mitochondrium (M). Note the pellicle on the periphery of the cell. **23.** A vegetative cell surrounded by 2 pellicles. **24.** A vegetative cell surrounded by 2 pellicles, one of which is rupturing to release a cell with 1 pellicle. **25–30.** Autosporulation process. **25.** A typical vegetative cell with a characteristic long mitochondrium (M), Golgi (G), and a nucleus (N). **26.** Cell division producing 2 daughter cells within the pellicle. **27.** Each of the daughter cells formed their own pellicles while the old pellicle ruptures to release the fully matured daughter vegetative cells. **28.** Cell division resulting in the formation of 4 (one is not in the plane of the section) daughter cells within the old pellicle. **29.** Cell division resulting in the formation of 8 (one is not in the plane of the section) daughter cells within the old pellicle. **30.** Release of fully mature daughter vegetative cells from the ruptured pellicle of the original mother cell.

Table **2.** Numbers of SjHe *Helicosporidium* cells produced per microliter of hemolymph and occurrence of cyst formation in 2 different noctuid hosts at 26 °C after injection of 5,000 or 50,000 vegetative cells per larva.

Host	Time after injection (d)	n	Helicosporidia (cells/µl hemolymph)[a]	Percentage of ICF	Relative amount of cysts (%) in ICF
Spodoptera exigua	1	18	2,764 ± 554a	0	NA
	2	18	48,211 ± 8,586ab	0	NA
	3	18	261,292 ± 61,729b	0	NA
	4	18	698,556 ± 80,865c	33	4 ± 1a
	5	12	909,167 ± 251,499c	75	14 ± 2b
	6	18	1,677,222 ± 206,258d	100	15 ± 2b
	8	14	1,965,000 ± 141,642d	100	21 ± 3c
Helicoverpa zea	1	9	411 ± 95a	0	NA
	2	9	7,678 ± 1,933a	0	NA
	3	9	78,233 ± 23,392a	0	NA
	4	9	1,311,667 ± 411,212a	0	NA
	5	9	6,324,444 ± 1,573,585b	67	6 ± 2a
	6	9	4,842,778 ± 715,976b	89	11 ± 1b
	8	9	5,983,333 ± 738,711b	100	15 ± 2cd
	10	9	6,777,778 ± 402,605b	100	15 ± 1cd
	12	9	9,727,778 ± 755,816c	100	18 ± 3d
	14	9	9,505,556 ± 711,973c	100	11 ± 2bc

Means (± SE) are based on 3 replicate assays with 2 or 3 replicate insects per time interval per host species per dosage.
[a]Within each host species means followed by a different letter are significantly different ($P \leq 0.05$, proc mixed and lsmeans).
ICF, insects with cyst formation; lsmeans, SAS least square means statement; proc mixed, procedure for mixed linear models; NA, not applicable.

Helicosporidium generally produced 2, 4, or 8 daughter cells per mother cell. Release from the mother cell pellicle occurred from each of these stages. The majority of vegetative cells, however, existed as single-cell stages and many of these cells underwent shedding of the pellicle without replication. The biological significance of this shedding process remains unknown.

Prolonged, periodic transfers of vegetative cell cultures of *Helicosporidium* induced palmelloid colony formation. The term palmelloid refers to the formation of non-motile, adherent cells that form a multicellular cluster. Palmelloid colonies in concert with abnormal cell wall formation at suboptimal growth conditions have been reported from several *Chlamydomonas* species, green algae of the class Volvocales that also exhibit vegetative replication via autosporulation (Nakamura, Bray, and Wagenaar 1975; Vallon and Wollman 1995; Visviki and Santikul 2000). Palmelloids cells of *Chlamydomonas eugametos* were much smaller (4–8 µm) than mature normal cells (10–12 µm) and TEM observations revealed no apparent abnormalities of cytoplasmic organelles; the existence of multilayered cell walls, however, indicated the inability of the cells to separate after autosporogenic cell division (Nakamura et al. 1975). In *Chlamydomonas reinhardti*, the formation of multicellular aggregates was shown to be caused by a mutation affecting *O*-glycosylation resulting in both a delayed degradation of the mother cell wall and an increased adhesion between daughter cell walls (Vallon and Wollman 1995).

Attempts to induce morphogenesis of the infectious cyst stage of *Helicosporidium* in vitro have failed. However, injection of in vitro-produced vegetative cells into the hemocoels of experimental noctuid hosts always resulted in the production of a normal complement of cysts. These findings clearly demonstrate that the in vitro cells were competent but lacked host-derived inputs to stimulate cyst differentiation. From the presented in vitro data, density dependence or media depletion could be excluded as main factors inducing cyst morphogenesis in *Helicosporidium*. It is not clear whether cyst differentiation first occurred intracellularly

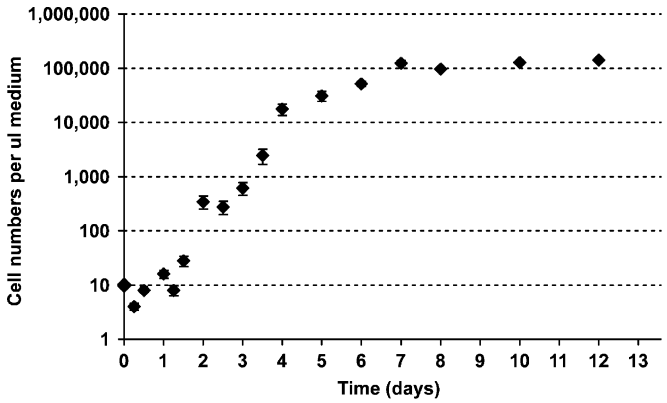

Fig. **31.** In vitro replication rates of isolate SjHe of *Helicosporidium* at 26 °C in cultures starting with 5,000 cells per 500-µl medium. Means (± SE) are based on 5 replicate assays with triplicate readings at different time points.

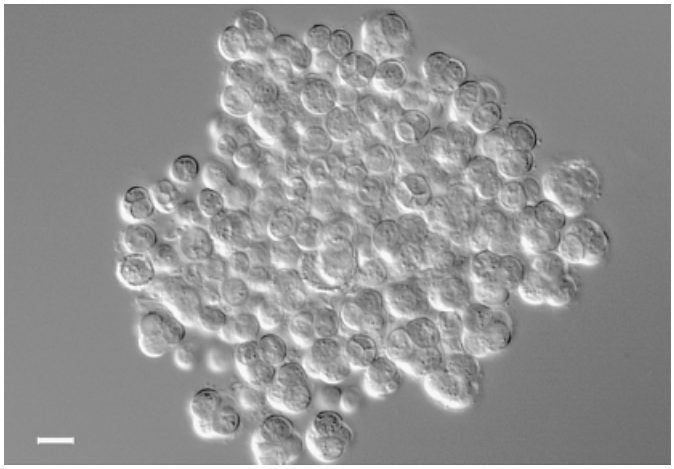

Fig. **32.** Cluster of vegetative cells of isolate SjHe of *Helicosporidium* after several transfers in tissue culture medium forming a palmelloid colony type. Scale bar = 5 µm.

(within hemocytes) or extracellularly in the host hemolymph. In the reported in vivo experiments, 15–21% of the *Helicosporidium* cells produced in 2 different host insects after injection of in vitro-produced vegetative cells differentiated into cysts (Table 2). After the death of the host, vegetative cell replication appeared to continue for 2–4 days but the cyst ratio decreased to 11%. In parallel in vitro experiments using the same preparations of vegetative cells, 23% of 4-cell stages were produced during the exponential phase of replication; once the stationary phase of in vitro replication was reached, 4-cell stages accounted for 14% of the cell population. We hypothesize that cysts originate from vegetative 4-cell stages, which are produced at a genetically determined ratio and require host-derived signals to induce cyst morphogenesis. However, in different bioassays, where larvae of *S. exigua* were infected per os with in vivo-produced cysts (as opposed to the injection of in vitro-produced vegetative cells), up to 39% cyst formation was observed within 10 d after the treatment (Bläske-Lietze and Boucias 2005). Potential factors inducing cyst differentiation in the host hemolymph are currently under investigation.

In the present study, cyst formation was not increased as a response to death of the host insect. This scenario could have been expected as a mechanism of efficient disease transfer within a host population, as the cuticle of a heavily infected, dead insect is easily disrupted, facilitating the release of cysts after death. However, the absolute numbers of cysts produced per microliter of hemolymph of an infected insect were considerably high (up to 10^6 in *H. zea*). Thus, infected hosts could be regarded as a large reservoir of infectious cysts that will eventually be released into the environment. The physiological changes inducing degradation of the host's cuticle and epidermis have not been examined for this pathogen. *Helicosporidium* infection does not cause liquefaction or mummification, which is typically observed as a postmortem result of certain viral and bacterial or fungal infections of insects, respectively (Boucias and Pendland 1998; Hom et al. 2002; Katsuma et al. 2004). The factors involved in maintenance of the disease within a population of susceptible hosts are yet to be investigated. Although transmission of helicosporidial infection from parental to filial generation has been reported in a heterologous host, *S. exigua* (Bläske and Boucias 2004), the low incidence of infection (2–5%) in the F1 progeny as well as the lack of association between *Helicosporidium* and reproductive organs of infected adults (Bläske-Lietze, Boucias, and Botts, pers. observ.) makes vertical transmission an unlikely mode of efficient disease transmission in nature. Transmission might be dependent on aquatic environments, as the majority of natural hosts (i.e. different species of mosquitoes and black flies) have at least one aquatic life stage, whereas other reported hosts are closely associated with ''aquatic'' microenvironments, such as plant sap, which could form a potential reservoir for released *Helicosporidium* cysts (Kellen and Lindegren 1973; Weiser 1970; Yaman and Radek 2005). *Helicosporidium* cysts have also been isolated from pond water (Avery and Undeen 1987).

The massive multiplication of this pathogen observed in the host hemolymph indicates that vegetative cells are able to avoid or suppress the cellular immune response of the host. The underlying mechanisms, however, are not known. In our experiments, hemocyte numbers in larvae and pupae of *H. zea* stayed constant during the course of helicosporidial infection and did not differ between infected and uninfected insects. It is known that certain hemolymph-borne parasites can affect the cellular immune response of their hosts by reducing or altering the activity of hemocytes. For example, infection of *S. exigua* larvae with the mycopathogen, *Beauveria bassiana*, significantly reduced numbers of circulating hemocytes and impaired phagocytosis (Hung and Boucias 1992). *Metarhizium anisopliae*, another entomopathogenic fungus, and *B. bassiana* have been shown to release extracellular proteases that reduced the phagocytic ability and altered the morphology and cytoskeleton structure of plasmatocytes from the greater wax moth, *Galleria mellonella* (Griesch and Vilcinskas 1998).

ACKNOWLEDGMENTS

We would like to thank Karen Kelley and Lynda Schneider (ICBR-EM Core Lab, UFL, Gainesville, FL) for their advice in histological methods; Genie White, Jessica Noling, and Allison McGee for their technical assistance; Janice Col (Statistical Consulting Unit, Department of Statistics, UFL, IFAS, Gainesville, FL) for her statistical advice; and Aurelien Tartar for his critical and helpful comments on an earlier draft of the manuscript. This work was supported by a grant from the National Science Foundation (NSF, MCB-0131017). Florida Agricultural Experiment Station Journal Series No. R-10942.

LITERATURE CITED

Avery, S. W. & Undeen, A. H. 1987. The isolation of microsporidia and other pathogens from concentrated ditch water. *J. Am. Mosq. Control Assoc.*, **3**:54–58.

Beakes, G. W. & Glockling, S. L. 1998. Injection tube differentiation in gun cells of a *Haptoglossa* species which infects nematodes. *Fungal Genet. Biol.*, **24**:45–68.

Bigliardi, E. & Sacchi, L. 2001. Cell biology and invasion of the microsporidia. *Microb. Infect.*, **3**:373–379.

Bläske, V.-U. & Boucias, D. G. 2004. Influence of *Helicosporidium* spp. (Chlorophyta: Trebouxiophyceae) infection on the development and survival of three noctuid species. *Environ. Entomol.*, **33**:54–61.

Bläske-Lietze, V.-U. & Boucias, D. G. 2005. Pathogenesis of *Helicosporidium* sp. (Chlorophyta: Trebouxiophyceae) in susceptible noctuid larvae. *J. Invertebr. Pathol.*, **90**:161–168.

Borza, T., Popescu, C. E. & Lee, R. W. 2005. Multiple metabolic roles for the non-photosynthetic plastid of the green alga *Prototheca wickerhamii*. *Eukaryot. Cell*, **4**:253–261.

Boucias, D. G. & Pendland, J. C. 1998. Principles of Insect Pathology. Kluwer Academic Publishers, Boston.

Boucias, D. G., Becnel, J. J., White, S. E. & Bott, M. 2001. In vivo and in vitro development of the protist *Helicosporidium* sp. *J. Eukaryot. Microbiol.*, **48**:460–470.

Chapman, H. C., Woodward, D. B. & Petersen, J. J. 1967. Pathogens and parasites in Louisiana Culicidae and Chaoboridae. *Proc. N.J. Mosq. Exterm. Assoc.*, **33**:54–60.

Conklin, T., Bläske-Lietze, V.-U., Becnel, J. J. & Boucias, D. G. 2005. Infectivity of two isolates of *Helicosporidium* spp. (Chlorophyta: Trebouxiophyceae) in heterologous host insects. *Fla Entomol.*, **88**:431–439.

Dall, D. J. 1983. A theory for the mechanism of polar filament extrusion in the microsporidia. *J. Theoret. Biol.*, **105**:647–659.

de Koning, A. P. & Keeling, P. J. 2004. Nucleus-encoded genes for plastid-targeted proteins in *Helicosporidium*: functional diversity of a cryptic plastid in a parasitic alga. *Eukaryot. Cell*, **3**:1198–1205.

de Koning, A. P., Tartar, A., Boucias, D. G. & Keeling, P. J. 2005. Expressed sequence tag (EST) survey of the highly adapted green algal parasite, *Helicosporidium*. *Protist*, **156**:181–190.

Franzen, C., Müller, A., Hartmann, P. & Salzberger, B. 2005. Cell invasion and intracellular fate of *Encephalitozoon cuniculi* (Microsporidia). *Parasitology*, **130**:285–292.

Frixione, E., Ruiz, L., Cerbon, J. & Undeen, A. H. 1997. Germination of *Nosema algerae* (Microspora) spores: conditional inhibition by D_2O, ethanol and Hg^{2+} suggests dependence of water influx upon membrane hydration and specific transmembrane pathways. *J. Eukaryot. Microbiol.*, **44**:109–116.

Fukuda, T., Lindegren, J. E. & Chapman, H. C. 1976. *Helicosporidium* sp. a new parasite of mosquitoes. *Mosq. News*, **36**:514–517.

Glauert, A. M. 1975. Fixation, Dehydration and Embedding of Biological Specimens. North-Holland Publishing Company, Amsterdam.

Gockel, G. & Hachtel, W. 2000. Complete gene map of the plastid genome of the non-photosynthetic euglenoid flagellate *Astasia longa*. *Protist*, **151**:347–351.

Griesch, J. & Vilcinskas, A. 1998. Proteases released by entomopathogenic fungi impair phagocytic activity, attachment and spreading of plasmatocytes isolated from haemolymph of the greater wax moth *Galleria mellonella*. *Biocontrol Sci. Technol.*, **8**:517–531.

Hembree, S. C. 1979. Preliminary report of some mosquito pathogens from Thailand. *Mosq. News*, **39**:573–582.

Hom, L. G., Ohkawa, T., Trudeau, D. & Volkman, L. E. 2002. *Autographa californica* M nucleopolyhedrovirus ProV-CATH is activated during infected cell death. *Virology*, **296**:212–218.

Hung, S.-Y. & Boucias, D. G. 1992. Influence of *Beauveria bassiana* on the cellular defense response of the beet armyworm, *Spodoptera exigua*. *J. Invertebr. Pathol.*, **60**:152–158.

Huss, V. A. R., Ciniglia, C., Cennamo, P., Cozzolino, S., Pinto, G. & Pollio, A. 2002. Phylogenetic relationships and taxonomic position of *Chlorella*-like isolates from low pH environments (pH < 30). *BMC Evol. Biol.*, **2**:13.

Katsuma, S., Tanaka, S., Shimada, T. & Kobayashi, M. 2004. Reduced cysteine protease activity of the hemolymph of *Bombyx mori* larvae infected with *fp25K*-inactivated *Bombyx mori* nucleopolyhedrovirus results in the reduced postmortem host degradation. *Arch. Virol.*, **149**:1773–1782.

Keilin, D. 1921. On the life-history of *Helicosporidium parasiticum*, n. g., n. sp., a new type of protist parasitic in the larva of *Dasyhelea obscura* Winn. (Diptera, Ceratopogonidae) and in some other arthropods. *Parasitology*, **13**:97–113.

Kellen, W. R. & Lindegren, J. E. 1973. New host record for *Helicosporidium parasiticum*. *J. Invertebr. Pathol.*, **22**:296–297.

Knauf, U. & Hachtel, W. 2002. The genes encoding subunits of ATP synthase are conserved in the reduced plastid genome of the heterotrophic alga *Prototheca wickerhamii*. *Mol. Genet. Genomics*, **267**: 492–497.

Köhler, W., Schachtel, G. & Voleske, P. 1992. Biostatistik. Einführung in die Biometrie für Biologen und Agrarwissenschaftler. Springer, Berlin.

Lindegren, J. E. & Okumura, G. T. 1973. Pathogens from economically important nitidulid beetles. *USDA ARS*, **W-9**:1–7.

Lindegren, J. E. & Hoffmann, D. F. 1976. Ultrastructure of some developmental stages of *Helicosporidium* sp. in the navel orangeworm, *Paramyelosis transitella*. *J. Invertebr. Pathol.*, **27**:105–113.

Mead, G. P., Ratcliffe, N. A. & Renwrantz, L. R. 1986. The separation of insect haemocyte types on Percoll gradients; methodology and problems. *J. Insect Physiol.*, **32**:167–177.

Nakamura, K., Bray, D. F. & Wagenaar, E. B. 1975. Ultrastructure of *Chlamydomonas* eugametos palmelloids induced by chloroplatinic acid treatment. *J. Bacteriol.*, **121**:338–343.

Neter, J., Wasserman, W. & Kutner, M. H. 1990. Applied Linear Statistical Models: Regression, Analysis of Variance, and Experimental Designs. Richard Irwin Inc., Illinois.

Pleshinger, J. & Weidner, D. 1985. The microsporidian spore invasion tube. IV. Discharge activation begins with pH-triggered Ca^{2+} influx. *J. Cell Biol.*, **100**:1834–1838.

Pore, R. S. 1985. *Prototheca* taxonomy. *Mycopathologia*, **90**:129–139.

Poyton, R. O. & Branton, D. 1972. Control of daughter cell number variation in multiple fission: genetic versus environmental determinants in *Prototheca*. *Proc. Natl. Acad. Sci. USA*, **69**:2346–2350.

Purrini, K. 1980. On the incidence and distribution of parasites of soil fauna of mixed coniferous forests, mixed leaf forests, and pure beech forests of lower Saxony, West Germany. *Proc. 7th Int. Colloq. Soil Zool.*, 561–582.

Purrini, K. 1985. On disease agents of insect pests of wild palms and forests in Tanzania. *Z. Angew. Entomol.*, **99**:237–240.

Rao, P. V. 1998. Statistical Research Methods in the Life Sciences. Duxbury Press, Pacific Grove.

SAS. 1999. User's Guide, Version 8.0. SAS Institute, Cary, NC.

Seif, A. I. & Rifaat, M. M. A. 2001. Laboratory evaluation of a *Helicosporidium* sp. (Protozoa: Helicosporidia) as an agent for the microbial control of mosquitoes. *J. Egyptian Soc. Parasitol.*, **31**:21–35.

Shorey, H. H. & Hale, R. C. 1965. Mass rearing of the larvae of nine noctuid species on a simple artificial medium. *J. Econ. Entomol.*, **58**: 522–524.

Tartar, A. & Boucias, D. G. 2004. The non-photosynthetic, pathogenic green alga *Helicosporidium* sp. has retained a modified, functional plastid genome. *FEMS Microbiol. Lett.*, **233**:153–157.

Tartar, A., Boucias, D. G., Becnel, J. J. & Adams, B. J. 2003. Comparison of plastid 16S rRNA (rrn16) genes from *Helicosporidium* spp.: evidence supporting the reclassification of Helicosporidia as green algae (Chlorophyta). *Int. J. Syst. Evol. Microbiol.*, **53**:1719–1723.

Undeen, A. H. & Van der Meer, R. K. 1994. Conversion of intrasporal trehalose into reducing sugars during germination of *Nosema algerae* (Protista: Microspora) spores: a quantitative study. *J. Eukaryot. Microbiol.*, **41**:129–132.

Vallon, O. & Wollman, F.-A. 1995. Mutations affecting *O*-glycosylation in *Chlamydomonas reinhardtii* cause delayed cell wall degradation and sex-limited sterility. *Plant Physiol.*, **108**:703–712.

Visviki, I. & Santikul, D. 2000. The pH tolerance of *Chlamydomonas applanta* (Volvocales, Chlorophyta). *Arch. Environ. Contam. Toxicol.*, **38**:147–151.

Weiser, J. 1970. *Helicosporidium parasiticum* Keilin infection in the caterpillar of a hepialid moth in Argentina. *J. Protozool.*, **17**: 440–445.

Wilson, R. J. 2005. Parasite plastids: approaching the endgame. *Biol. Rev. Cambridge Philos. Soc.*, **80**:129–153.

Wong, A. & Beebee, T. 1994. Identification of a unicellular, non-pigmented alga that mediates growth inhibition in anuran tadpoles: a new species of the genus *Prototheca* (Chlorophyceae: Chlorococcales). *Hydrobiologia*, **277**:85–96.

Yamamoto, M., Nozaki, H., Miyazawa, Y., Koide, T. & Kawano, S. 2003. Relationship between presence of a mother cell wall and speciation in the unicellular microalga *Nannochloris* (Chlorophyta). *J. Phycol.*, **39**:172–184.

Yaman, M. & Radek, R. 2005. *Helicosporidium* infection of the great European spruce bark beetle, *Dendroctonus micans* (Coleoptera: Scolytidae). *Eur. J. Protistol.*, **41**:203–207.

Younger, M. S. 1998. SAS® Companion for P.V. Rao's Statistical Research Methods in the Life Sciences. Duxbury Press, Pacific Grove.

Received: 09/20/05, 12/22/05; accepted: 12/22/05